Wagging and torsion vibronic structure in the T1 ← So electronic spectrum of acetaldehyde

ARTICLE *in* THE JOURNAL OF PHYSICAL CHEMISTRY B · APRIL 2002

Impact Factor: 3.3 · DOI: 10.1021/j100057a001

The Journal of Physical Chemistry

 VOLUME 98, NUMBER 6, FEBRUARY 10, 1994

ARTICLES

Wagging and Torsion Vibronic Structure in the $T_1 \leftarrow S_0$ Electronic Spectrum of Acetaldehyde

Alfonso Niño and Camelia Muñoz-Caro

E.U. Informática de Ciudad Real, Universidad de Castilla la Mancha, Ronda de Calatrava s/n, 13071 Ciudad Real, Spain

David C. Moule*

Department of Chemistry, Brock University, St. Catharines, Ontario, L2S 3A1 Canada

*Received: August 30, 1993; In Final Form: October 22, 1993**

The $T_1 \leftarrow S_0$ electronic band spectrum in acetaldehyde was simulated from RHF and UHF/MP2/6-311G(d,p) *ab initio* calculations for the two electronic states. The torsion-wagging energy levels were evaluated by the variational method using free rotor basis functions expressed as symmetrized double-Fourier expansions. A comparison of the calculated band spectrum to the long-path absorption spectrum allowed for the assignment of a number of clearly defined bands and placed the origin at 27 240 cm^{-1}. The calculated height of the barrier to internal rotation for the lower S_0 state of 415 cm^{-1} yielded levels in excellent agreement with the torsional levels derived from far infrared measurements. The calculated T_1 excited-state barrier heights for the pure torsion and wagging motions were 647 and 968 cm^{-1}. The corresponding values in the S_1 state are 709 and 776 cm^{-1}.

Introduction

The search for an accurate description of large-amplitude vibrations is of interest from both a theoretical and an experimental point of view. Large-amplitude motions are controlled by intramolecular interactions. Upon electronic excitation, the change in electronic structure produces a change in the potentials that govern the large-amplitude motions. These changes in structure result in complicated vibronic patterns in the electronic spectra.

Acetaldehyde is the prototype for the aliphatic series of carbonyl compounds. In the S_0 ground state, the torsion of the methyl group is the single large-amplitude motion. The most stable equilibrium conformation has a planar heavy-atom frame with one of the methyl hydrogens eclipsing the carbonyl oxygen.[1-6] Upon $n \rightarrow \pi^*$ electronic excitation, in accordance with Walsh's rules,[7] the molecule experiences a pyramidalization at the carbonyl moiety. At the opposite end of the molecule the preference of the methyl group changes from an eclipsed to a staggered conformation.[8] Thus, two large-amplitude motions are present in the first singlet, S_1, and triplet, T_1, excited states: the torsion of the methyl group, Q_{15}, and the wagging of the aldehydic hydrogen, Q_{14}. These changes in conformation produce long progressions in the $S_1 \leftarrow S_0$ and $T_1 \leftarrow S_0$ electronic spectra. In contrast to the $S_1 \leftarrow S_0$ electronic spectrum where the Herzberg–Teller transitions play a dominant role, the $T_1 \leftarrow S_0$ spectrum arises from spin–orbit coupling to higher electronic states. Both the intensity and the direction of the transition moment are borrowed or stolen from allowed transitions to higher electronic states. Thus, the vibronic selection rules in a singlet–triplet spectrum are controlled by the Franck–Condon principle. The spin–orbit coupling in the carbonyl group is weak, and the singlet–triplet transitions have low oscillator strength. High gas pressure and long path lengths are necessary for absorption studies.[9,10] The laser-induced phosphorescence excitation spectrum, LIP, has not been observed and is probably complicated by the longer lifetime of the triplet state.

* Abstract published in *Advance ACS Abstracts*, December 15, 1993.

0022-3654/94/2098-1519$04.50/0

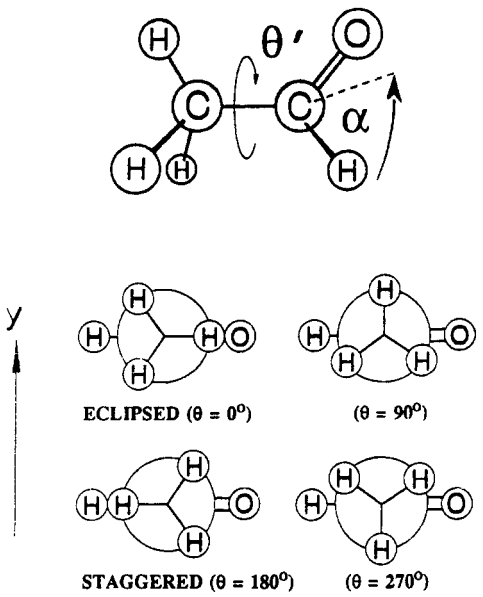

Figure 1. Molecular structure of acetaldehyde showing the torsional, θ', and wagging, α, angles. The Newman projections define the generalized θ coordinate.

In a previous study a variational technique was proposed for the study of large-amplitude vibrations and was applied to the case of torsion and wagging in the S_1 state of acetaldehyde.[11] In the present paper we use this methodology for the analysis of the vibronic structure of the highly congested $S_0 \rightarrow T_1$ electronic absorption spectrum of acetaldehyde.

Methodology

Since torsion and wagging motions exhibit large-amplitude displacements in the T_1 state, it is necessary to obtain the potential energy surface as a function of the methyl torsional, θ', and wagging, α, coordinates. Thus, the nuclear potential energy is evaluated for a grid of points in the θ' and α angles which are defined in Figure 1. In our previous study of the $S_1 \leftarrow S_0$ spectrum of acetaldehyde, we found electronic correlation energy to be important in describing the wagging potential in the first singlet excited state.[11] In this study, correlation energy is accounted for by using the MP2 approximation of many-body perturbation theory. The triple-ζ split plus polarization 6-311G(d,p) basis set developed for the MP2 level[12] was selected. The RHF approximation was used for the ground state, and the UHF approximation was used for the first triplet excited state. A fully relaxed model was used for the description of the torsion and wagging motions. Thus, the molecular structure was optimized for each grid point at the all-electron (full) MP2 level with the BERNY conjugate gradient algorithm.[13] The equilibrium geometries obtained for the S_0 and the S_1 states with the 4-31G(d,p) basis[14] were used as the starting point for the optimization of the S_0 and T_1 states, respectively. All computations were carried out by means of the GAUSSIAN 90 package.[15]

The acetaldehyde molecule can be classified by the G_6 nonrigid group[16] that is isomorphic to C_{3v}. This group accounts for the rotation of the methyl moiety and the simultaneous inversion of the torsional and wagging vibrations through the cyclic permutation of the hydrogens and the change of sign in Θ' and α coordinates, respectively. The potential energy functions were obtained by fitting the energy points to a double-Fourier series expansion in θ and α of A_1 symmetry. The torsional part of the potential functions may be described as a truncated Fourier expansion of adapted symmetry. Thus, for a planar frame we have

$$V(\theta) = \sum_{i=0}^{n} A_i(\cos(3i\theta)) \tag{1}$$

However, it is important to realize that the θ coordinate appearing in the potential function is a generalized coordinate related to, but not equivalent to, the torisonal coordinate θ'. The usual approximation, $\theta = \theta'$, is valid only when the methyl top is symmetric, with hydrogens separated by dihedral angles of 120°. In this case, the summation in eq 1 runs until $i = 1$. In the general case, however, the effect of the remaining $3N - 7$ vibrations on the rotating methyl group breaks the threefold symmetry of the θ' coordinate and the hydrogens now are separated by dihedral angles that differ from 120°. In this last case, the summation in eq 1 runs usually until $i = 2$ or 3. In this study we have used a generalized coordinate, θ, defined by its physical behavior in the following way: the eclipsed and staggered planar conformations of acetaldehyde were taken to be $\theta = 0°$ and $\theta = 180°$, respectively. The conformations with a methyl hydrogen atom perpendicular to the molecular frame pointing up or down are defined as $\theta = 90°$ and $\theta = 270°$, respectively (see Figure 1).

The Hamiltonian for the nuclear motion was solved by the variational principle using free rotor basis functions. The kinetic energy elements were obtained using the rovibrational G matrix[17,18] with the KICO[19] program for each of the fully optimized geometries. The results were fitted to double-Fourier expansions of A_1 adapted symmetry. In our two-dimensional case, the kinetic and potential terms for each element of the Hamiltonian matrix become

$$\langle \varphi_m|\hat{T}|\varphi_n\rangle = \sum_{i}^{2}\sum_{j}^{2}\sum_{k}^{N_B} B^0_{ijk}[\langle f_{mi}|f_{ijki}|f'_{ni}\rangle \langle f_{mj}|f_{ijkj}|f'_{nj}\rangle + \langle f_{mi}|f'_{ijki}|f_{ni}\rangle \langle f_{mj}|f_{ijkj}|f'_{nj}\rangle] \prod_{p\neq i,j}^{2} \langle f_{mp}|f_{ijkp}|f_{np}\rangle \tag{2}$$

for $i \neq j$, whereas for $i = j$ we have

$$\langle \varphi_m|\hat{T}|\varphi_n\rangle = \sum_{i}^{2}\sum_{k}^{N_B} (B^0_{iik}[\langle f_{mi}|f_{iiki}|f''_{ni}\rangle + \langle f_{mi}|f'_{iiki}|f'_{ni}\rangle] \prod_{p\neq i}^{2} \langle f_{mp}|f_{iikp}|f_{np}\rangle) \tag{3}$$

The potential energy part is obtained as

$$\langle \varphi_m|\hat{V}|\varphi_n\rangle = \sum_{i}^{N_V} V^0_i \prod_{p}^{2} \langle f_{mp}|f_{ip}|f_{np}\rangle \tag{4}$$

where N_B and N_V represent the number of terms in the expansions for the kinetic and potential functions. The basis functions are represented by f:

$$f_{ij} = \begin{cases} \dfrac{1}{\sqrt{\pi}}\cos(N\alpha_j) & \\ & \text{for } N = 1, 2, \ldots \\ \dfrac{1}{\sqrt{\pi}}\sin(N\alpha_j) & \\ \dfrac{1}{\sqrt{2\pi}} & \text{for } N = 0 \end{cases} \tag{5}$$

In the present case only the Franck–Condon transitions are taken into account. Thus, the transition dipole moment between the vibrational states n and m is taken to be constant, and the

TABLE 1: Comparison of Theoretical and Experimental Torsional Barriers, in cm^{-1}, in the S_0 Ground State of Acetaldehyde

source	barrier
RHF/MP2/6-311G(d,p)	415.2
RHF/4-31G(d,p)	378.8[a]
RHF/6-31G(d,p)	373.8[b]
RHF/MP2/6-31G(d,p)	364.1[b]
IR-microwave measurements	407.9[c]
infrared measurements	408.6[d]

[a] Reference 14. [b] Reference 21. [c] Reference 22. [d] Reference 23.

relative intensities are calculated as

$$I \propto (g_n - g_m)\mu^2_{nm} \tag{6}$$

where g represents the population for each vibrational level and μ_{nm} is

$$\mu_{nm} = \sum_i^{N_F}\sum_l^{N_F} C_{in}C_{lm}\prod_p^2 \langle f_{ip}|f_{lp}\rangle \tag{7}$$

which, from the orthogonality of the basis functions, can be taken to the simpler form

$$\mu_{nm} = \sum_i^{N_F} C_{in}C_{im} \tag{8}$$

with c_{ln}, c_{lm} being the coefficients of the wave functions. This variational technique was applied with the ROVI program.[20]

Results and Discussion

S_0 Ground State. Our two-dimensional study, as expected, predicts the equilibrium conformation to be the planar eclipsed structure of Figure 1. The barrier to methyl torsion is compared in Table 1 with previous theoretical and experimental values. The present value of 415.2 cm^{-1} is in excellent agreement with the recent experimental results of 407.9 cm^{-1} (high-resolution infrared and microwave analysis for the $v = 0$–2 torsional states[22]) and 408.6 cm^{-1} (infrared torsional frequencies[23]). The excellent agreement can be attributed to the higher flexibility of the triple-ζ split basis and to the meshing of the 6-311G(d,p) basis set to the MP2 approximation.

The grid of energy points was fit to a symmetry-adapted double-Fourier expansion of A_1 symmetry in the θ and α coordinates. This expression shows the potential as a series of trigonometric terms. This form is very useful from a computational point of view particularly when describing several vibrations. The same procedure was used in the expansion of the B_θ, B_α, and $B_{\theta\alpha}$, torsional, wagging, and kinetic coupling terms. The results are shown in Table 2. It is clear that terms in 6θ make a significant contribution to the potential as a result of the nonsinusoidal variation with respect to the θ coordinate. The 3θ and 6θ terms describe the height and the width of the torsional barrier.

TABLE 3: Observed and Calculated Torsional and Wagging Levels, in cm^{-1}, for the S_0 State of Acetaldehyde

v_{15}	v_{14}	sym.	calc[a]	calc[b]	calc[c]	obs
0	0	a_1	0.00	0.00	0.00	0.00
		e	0.10	0.06	0.08	0.0690
1	0	e	139.28	147.61	141.43	141.9935[d]
		a_2	142.04	149.35	143.37	143.7434[d]
2	0	a_1	239.66	262.38	252.96	255.2243[d]
		e	258.08	276.66	267.77	269.1121[d]
3	0	e	328.15	355.88	346.45	349.22[e]
		a_2	397.26	416.72	407.80	408.31[e]
4	0	a_1	405.54	432.24	423.45	425.64[e]
		e	496.37	517.46	508.86	508.99[e]
0	1	a_2			936.2	764.1[f]
		e			936.3	764.1[f]

[a] Reference 23. [b] This work, one-dimensional calculation. [c] This work, two-dimensional calculation. [d] Reference 22. [e] Reference 21 (calculated from the potential obtained by fitting the experimental data for the torsional $v = 0$–2 levels). [f] Reference 24.

Torsional and wagging energy levels were obtained from the expansion coefficients of Table 2. The results are shown in case c of Table 3 where they are compared with the literature value. The differences between the observed and calculated torsional levels, including those above the barrier, range from 0.37 to 2.26 cm^{-1}. There is also a good agreement between the experimental values of Belov *et al.*[22] (1.75/13.89 cm^{-1}) and theoretical values (1.94/14.81 cm^{-1}) of the A–E symmetry splittings of the torsional $v = 1$ and 2 levels.

To gain further insight into the role of wagging coupling, we performed a one-dimensional calculation in the torsional coordinate. *Ab initio* energy data points and fully optimized geometries for the $\theta = 0$, 90, 180, and 270° conformations in the wagging equilibrium position $\alpha = 0°$ were used for the torsional potential and the B_0 kinetic terms which are shown in Table 2. The one-dimensional torsional levels are collected in case b of Table 3 and are compared with the literature values.

Our predicted levels for the two-dimensional case are considerably better than the one-dimensional results. In particular, we found A–E splittings of 1.74/14.28 cm^{-1} for the first two torsional levels. The improvement over the 2.76/18.42 cm^{-1} values of Ozkabak *et al.*[21] can be attributed to the definition of the generalized coordinate θ and to the value for the torsional barrier. The success of the two-dimensional case can be explained by an analysis of the double-Fourier expansion of the potential energy shown in Table 2 where the (cos)(cos) and (sin)(sin) coupling

TABLE 2: Fits of the Potential and Kinetic Terms, in cm^{-1}, of the S_0 Ground State of Acetaldehyde Including Correlation and Standard Deviation

term	$V(\theta,\alpha)^a$	$B_\theta{}^a$	$B_\alpha{}^a$	$B_{\theta\alpha}{}^a$	$V(\theta)^b$	$B(\theta)^b$
cte	28337.66	8.9183	16.3606	–4.2709	205.86	7.6437
cos(α)	–30989.43		5.2502	–0.7858		
cos(2α)	2857.51	0.0766		–0.4282		
cos(3α)		0.0286	0.1836			
cos(3θ)	213.48	–0.0555	–0.0081	0.0551	–207.62	0.0305
cos(6θ)	–11.77	0.0026			1.76	0.0037
cos(6θ)cos(α)			0.0019	–0.0019		
cos(3θ)cos(2α)	–432.63	0.1451	0.0830	–0.1632		
cos(3θ)cos(3α)	11.36	–0.0134	0.0406			
cos(6θ)cos(3α)	13.82					
sin(3θ)sin(α)	–86.83	–0.0152				
sin(3θ)sin(2α)	433.15		–0.0149			
sin(3θ)sin(3α)		0.0326	0.0515	–0.0442		
R	1.0000	0.9994	1.0000	1.0000	1.0000	1.0000
σ (cm^{-1})	1.3115	0.0021	0.0023	0.0020	0.0000	0.0000

[a] Two-dimensional case. [b] One-dimensional case.

TABLE 4: Comparison of Theoretical and Experimental Torsional and Inversion Barriers, in cm^{-1}, for the T_1 State of Acetaldehyde

source	torsion barrier	inversion barrier
UHF/MP2/6-311G(d,p)	647.4	968.1
UHF/6-31+G(d)		874.4[a]
CIS/6-31+G(d)		1112.7[a]
Moule and Ng[b]	624.8 ± 21.5	
Yakovlev and Godunov[c]	590	1110

[a] Calculated from the data of ref 6. [b] Reference 9. [c] Reference 10.

TABLE 5: Fits of the Potential and Kinetic Terms, in cm^{-1}, of the First Triplet T_1 State of Acetaldehyde Including Correlation and Standard Deviation

term	$V(\theta,\alpha)^a$	$V(\theta,\alpha)^b$	$B_\theta{}^a$	$B_\alpha{}^a$	$B_{\theta\alpha}{}^a$
cte	6584.54	6147.25	7.8629	18.9268	-3.0729
$\cos(\alpha)$	-7088.89	-6576.19			-0.6418
$\cos(2\alpha)$			-0.2191	1.8902	
$\cos(3\alpha)$	1632.88	1552.58	0.3370	0.1925	-0.3854
$\cos(3\theta)$	317.61	194.24	0.2392	0.0241	-0.0890
$\cos(6\theta)$	7.66				
$\cos(3\theta)\cos(\alpha)$			-0.3568		0.1332
$\cos(3\theta)\cos(2\alpha)$	-83.21	180.82	0.1095	-0.0765	
$\cos(3\theta)\cos(3\alpha)$	-59.83	-206.10		0.0666	-0.0379
$\cos(6\theta)\cos(\alpha)$		8.61	0.0020		-0.0041
$\sin(3\theta)\sin(\alpha)$	-168.54	184.82	0.1215	0.0476	-0.0710
$\sin(3\theta)\sin(2\alpha)$	95.72	-226.30	-0.0588		
$\sin(3\theta)\sin(3\alpha)$	111.17	214.25		-0.0256	0.0318
R	1.0000	1.0000	0.9989	0.9998	0.9997
σ (cm^{-1})	3.16	3.89	0.0063	0.0193	0.0093

[a] Obtained by fitting the calculated data. [b] Obtained from the quadratic-Gaussian potential.

terms are found to play an important role. These coefficients have a magnitude comparable to the pure torsional terms, $\cos(3\theta)$ and $\cos(6\theta)$. However, they are small when compared to the pure wagging, $\cos(\alpha)$ and $\cos(2\alpha)$, terms. In our fully relaxed model the effect of the optimization is to give an average over the molecular vibrations. Thus, the terms in the double-Fourier expansion do not reflect the wagging–torsion coupling but rather the correlation between the θ and α coordinates. The Fourier expansion describes the behavior of the *ab initio* potential surface. It does not represent a model for the torsion–wagging relationship. The effect is that the two-dimensional calculation represents the coupling of torsion to the other remaining vibrations better than does the one-dimensional model.

The first excited wagging level is calculated to lie at 936.3 cm^{-1}, which is higher than the experimental value[24] of 764.1 cm^{-1}. This result is not surprising because wagging in the S_0 state is not a large-amplitude coordinate and it cannot be isolated from the four other out-of-plane, high-frequency modes. In particular, it has been shown that the true wagging normal mode consists of 0.83 (aldehyde wag α) + 0.11 (CCH methyl wag) + 0.01 (HCH methyl wag).[25] This mixing of internal coordinates is responsible for the failure of our model to describe the wagging motion.

T_1 Triplet State. Global optimization shows that the most stable T_1 structure is pyramidal with a wagging angle of 39.66°. This angle is 2° higher than that of the S_1 state,[11,14] 37.83°. The methyl group is found to adopt a nearly staggered conformation with a torsion angle of 185.61°. The barriers for torsion and inversion are compared in Table 4 with the literature. A grid of energy points obtained from the *ab initio* calculations was fitted to a double-Fourier series of A_1 symmetry in a fashion similar to the ground state. The results are shown in Table 5 where it can be seen that three (sin)(sin) cogwheel coupling terms appear in the potential function. Thus, torsion–wagging coupling becomes important for the T_1 electronic state of acetaldehyde. Torsion+wagging energy levels are shown in Table 6 together with the experimental results. The patterns of levels which are found in Table 6 may be described as a set of manifolds of levels in the Q_{15} torsional mode attached to the inversion split levels of the Q_{14} wagging mode. The extent of coupling between the modes can be inferred from the inversion splittings between the wagging levels. For example, for the e components the ($0^- - 0^+$ inversion doubling) separations between the first three members of the torsional progression are 4.59, 0.60, and 1.55 cm^{-1}. The magnitudes of the splittings indicate that the barrier to aldehyde inversion is high; the variation in the intervals indicates that coupling between the two modes is substantial.

TABLE 6: Observed and Calculated Torsion and Wagging Levels, in cm^{-1}, for the T_1 State of Acetaldehyde

v_{15}	v_{14}	sym	calc[a]	calc[b]	obs
0	0	a_1	0.00	0.00	0.00[c]
		e	0.01	0.01	0.00[c]
1	0	e	182.90	181.15	179.8[d]
		a_2	183.21	181.49	179.8[d]
2	0	a_1	342.50	339.03	334.3[d]
		e	345.82	342.32	334.3[d]
3	0	e	471.12	465.92	
		a_2	498.51	494.18	
0	1	a_2	4.59	4.52	
		e	4.59	4.52	
1	1	e	183.50	181.62	
		a_1	183.58	181.72	
2	1	a_2	344.27	340.34	
		e	347.02	343.55	
3	1	e	476.69	470.73	
		a_1	494.97	490.60	
0	2	e	536.71	535.82	
		a_1	537.18	536.07	
1	2	e	743.81	738.72	
		a_2	744.31	739.65	
2	2	a_1	881.53	871.44	888.4[e]
		e	883.40	871.67	888.4[e]

[a] From the double-Fourier series expansion. [b] From the quadratic-Gaussian potential. [c] Not directly observed. [d] Reference 9. [e] Reference 10.

Assignments. The room-temperature $S_0 \rightarrow T_1$ spectrum recorded under long-path conditions by Moule and Ng[9] is extremely congested as a result of the activity in the torsion and wagging large-amplitude modes. In addition, hot bands from the companion $S_0 \rightarrow S_1$ system extend into the blue end of this system and strongly interfere. Thus, useful information can only be extracted from a small region on either side of the electronic origin. We have simulated the jet-cooled spectrum at 5 K. The spectrum is shown in Figure 2. The present calculations show that the strengths of transitions of the 0_0^0 origin band having intensities of 0.8(a_1) and 0.4(e) are too weak to be observed directly. To fix the position of the electronic origin, it was necessary to combine the observed hot intervals with the torsional levels of the S_0 state. By this technique the origin was placed at 27 240 cm^{-1}. From this starting point it was possible to locate a clearly defined band at +334.3 cm^{-1} which can be assigned to the a_1 and e components of the double quantum of methyl torsion, 15_0^2. From Table 6, the calculated positions of these bands are 342.5(a_1) and 345.8(e) cm^{-1} and their combined strengths are 20.2. The only other feature that can be correlated to the present calculations is the $14_0^2 15_0^2$ band, with intensity 100.0, which is predicted to appear at 881.5 cm^{-1}. Yakovlev and Godunov[10] locate a strong band with an interval of +888.4 cm^{-1} which can be given this assignment. Thus, the observed absorption system contains a dense structure, and the problem of band overlap and multiple assignments allows for a correlation only for a few key bands in the spectrum.

An important feature of this work is the shape of the T_1 torsion–wagging potential function and its relationship to the companion S_1 surface. The two parameters that can be correlated are the heights of the barriers to the one-dimensional torsional and wagging motions. For the T_1/S_1 states, the barriers to wagging

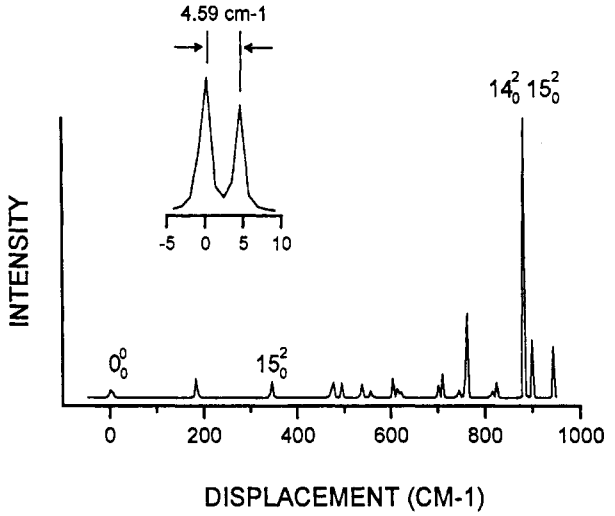

Figure 2. Low-temperature (5 K) $S_0 \rightarrow T_1$ simulated jet-cooled spectrum of acetaldehyde. The inset shows the 0_0^0 inversion splitting in the first torsional transition.

inversion are 968/776 cm^{-1}. Thus, the barrier in the wagging direction is greater in the T_1 state than it is in the corresponding S_1 state. This difference would be anticipated since the corresponding T_1/S_1 values for the molecular prototype CH_2O[8] are 775.6/350.0 cm^{-1}.

Somewhat more surprising are the nearly equal T_1/S_1 values of the barriers to torsion in the two states, 647/709 cm^{-1}. In the case of the single-rotor system methyl glyoxal,[26] the barriers to internal rotation are observed to be sensitive to spin interchange, with values 115/190 cm^{-1} for the T_1/S_1 states, respectively. For acetophenone,[27] the effect is even more dramatic with the T_1 and S_0 states adopting an eclipsed conformation and the S_1 state a staggered conformation. For systems where the C=O group conjugates with adjacent C=O or C=C groups, the barrier to methyl group rotation appears to be sensitive to spin interchange. For unconjugated systems such as acetaldehyde, the barriers to methyl rotation in the companion states are less strongly influenced by electron spin.

Alternative Quadratic-Gaussian Wagging Potential Function. An alternative form for the potential energy is a quadratic-Gaussian combination[28] for the wagging coordinate supplemented by a Fourier expansion for torsion. This approximation was successfully used for the S_1 state of acetaldehyde.[11] Thus, we obtain for torsion and wagging, respectively,

$$V(\theta) = A + B\cos(3\theta) + C\cos(6\theta) \quad (9)$$

$$V(\alpha) = A + B\alpha^2 + De^{-C\alpha^2} \quad (10)$$

To obtain a flexible two-dimensional potential that incorporates the simultaneous inversion of θ and α of the G_6 group, the above expressions were combined to yield

$$V(\theta,\alpha) = V(\theta)\,V(\alpha) \quad (11)$$

However, eq 11 does not account for the θ,α coupling. This coupling can be introduced as a factor that breaks the planar symmetry introduced by the θ coordinate. Thus, the $V_{\theta\alpha}$ coupling term can be expressed as

$$V_{\theta\alpha} = \cos(3\theta + f(\alpha)) \quad (12)$$

an expression that preserves the torsional threefold symmetry. The phase factor $f(\alpha)$ can be expanded in a Taylor series about the wagging coordinate

$$f(\alpha) = f_0 + (\partial f/\partial\alpha)_0\alpha + {}^1/_2(\partial^2 f/\partial\alpha^2)_0\alpha^2 + {}^1/_6(\partial^3 f/\partial\alpha^3)_0\alpha^3 \ldots \quad (13)$$

which, due to the necessary inversion invariance $V_{\theta\alpha}(-\theta,-\alpha) = V_{\theta\alpha}(\theta,\alpha)$, reduces to

$$f(\alpha) \simeq (\partial f/\partial\alpha)_0\alpha + {}^1/_6(\partial^3 f/\partial\alpha^3)_0\alpha^3 \quad (14)$$

where we retain up to the cubic term. Thus, a complete potential function can be obtained as

$$V(\theta,\alpha) = A + B\alpha^2 + De^{-C\alpha^2} + E\cos 3\theta + F\cos 6\theta + G\alpha^2\cos 3\theta + He^{-C\alpha^2}\cos 3\theta + K\alpha^2\cos 6\theta + Le^{-C\alpha^2}\cos 6\theta + M\cos(3\theta + a\alpha + b\alpha^3) \quad (15)$$

The exponential parameter C was obtained from a nonlinear set of equations for $\alpha = 0°$ (maximum), 15°, 40° (minimum), and 60° with $\theta = 180°$ (minimum). Once C was fixed, we solved another set of 12 nonlinear equations. The points considered are shown in Table 7. It can be seen that the zone around the global minimum and the wagging and torsional maxima and minima are well represented. The solution of the system of equations is shown in Table 8. As in the case of the S_1 state,[11] the quadratic-Gaussian potential was used for the double-Fourier expansion which is a more useful form for the computational calculation of energy levels. The fit is shown in case b of Table 5. The energy levels obtained with this approximation are shown in case b of Table 6. It can be observed that the difference from the previously calculated energy levels is of the order of several wavenumbers. It is interesting to note that the present case uses only half the number of the data points that were required for the original Fourier expansion.

TABLE 7: Potential Energy Points of the Quadratic-Gaussian Potential Function

α	θ	V (cm^{-1})	
0.00	0.00	1306.97	global max
0.00	90.00	1121.08	local max
0.00	180.00	968.10	local max
15.00	0.00	1104.40	local max
15.00	90.00	797.57	
15.00	180.00	694.20	
15.00	270.00	970.52	
37.00	0.00	660.84	local min
39.66	185.60	0.00	global min
37.66	90.00	239.23	local min
39.62	270.00	412.17	local min
60.00	180.00	996.19	

TABLE 8: Coefficients of the Quadratic-Gaussian Potential Function

coefficient[a]	value (cm^{-1})
constant	-5814.1900
α^2	1.4918
$\exp(-C\alpha^2)$	6943.5000
$\cos(3\theta)$	1562.5800
$\cos(6\theta)$	4.6637
$\alpha^2\cos(3\theta)$	-0.2131
$\exp(-C\alpha^2)\cos(3\theta)$	-1505.3800
$\alpha^2\cos(6\theta)$	-0.0013
$\exp(-C\alpha^2)\cos(6\theta)$	3.5638
$\cos(3\theta + a\alpha + b\alpha^2)$	112.2400

[a] With C = 0.000 383, a = -3.363 75, and b = 1.454 37D-05.

Conclusions

The near UV spectrum of acetaldehyde which is attributed to singlet–triplet n–π^* electron promotion is highly congested as a result of the activities of the methyl torsion and aldehyde wagging modes. Thus, a problem with the analyses has been to locate the electronic origin. The RHF/UHF calculations presented here appear to solve this problem in that they are able to reproduce semiquantitatively the key patterns in the band spectrum.

The MP2(full)/6-311G(d,p)//MP2(full)/6-311(d,p) barrier to methyl rotation in the S_0 state of 415.2 cm^{-1} is similar to the recent 412 cm^{-1} value of Leszczynski and Goodman.[29] These

authors show that the addition of polarization and correlation functions affects the barrier differently. They found that an increase in the number of polarization functions, 6-31G(d,p) to 6-311(3df,2p), increases the height of the barrier by about 100 cm^{-1} whereas the introduction of electron correlation, MP4-(SDTQ), reduces the barriers by 30 cm^{-1}.

The corresponding calculations for the upper T_1 state, UMP2/6-311G(d,p)//UMP2/6-311G(d,p) gave values of 647.4 and 968.1 cm^{-1} for the heights of the barriers to internal rotation and inversion. What is interesting is that the addition of polarization functions UMP2/6-311G(2d,p)//UMP2/6-311G(2d,p) reduces the heights of the corresponding barriers to 603.6 and 873.3 cm^{-1}. Diffuse functions in the basis UMP2/6-311+G(d,p)//UMP2/6-311+G(d,p) do not significantly alter the barrier to rotation, 644.2 cm^{-1}, whereas the inversion barrier falls to 887.8 cm^{-1}. Thus, the addition of polarization or diffuse functions to the T_1 UHF wave function has an effect on the barrier heights that is opposite to what is known for the S_0 state. Improving the electron correlation, from UHF/6-311(d,p)//UHF/6-311(d,p), 612.1 and 930.8 cm^{-1}, to UMP4/6-311(d,p)//UMP2/6-311(d,p), 633.8 and 965.9 cm^{-1}, increases the heights of the barriers. Again the direction of the change for the T_1 upper state is reverse to that found for the S_0 ground state.

The above calculations demonstrate that the problem of the *ab initio* determination of the barrier heights for the T_1 triplet state is not as complete as that of the S_0 ground state and that additional calculations at even higher levels of approximation should be carried out. The present results also suggest that further experimental studies are needed to firmly establish the torsion–wagging levels in the T_1 state.

Acknowledgment. A.N. and C.M.-C. wish to thank the Universidad de Castilla—La Mancha for financial support. D.C.M. acknowledges financial assistance from the Natural Sciences and Engineering Council of Canada.

Supplementary Material Available: Values of the energy levels for the S_0 and T_1 states and simulated jet-cooled spectrum at 5 K (transitions and intensities) (5 pages). Ordering information is given on any current masthead page.

References and Notes

(1) Kilb, R. W.; Lin, C. C.; Wilson, E. B., Jr. *J. Chem. Phys.* **1957**, *26*, 1695.
(2) Wiberg, K. B.; Martin, E. *J. Am. Chem. Soc.* **1985**, *107*, 5035.
(3) Crighton, J. S.; Bell, S. *J. Mol. Spectrosc.* **1985**, *112*, 285.
(4) Baba, M.; Hanazaki, I.; Nagashima, U. *J. Chem. Phys.* **1985**, *82*, 3938.
(5) Baba, M.; Nagashima, U.; Hanazaki, I. *J. Chem. Phys.* **1985**, *83*, 3514.
(6) Hadad, C. M.; Foresman, J. B.; Wiberg, K. B. *J. Phys. Chem.* **1993**, *97*, 4293.
(7) Walsh, A. D. *J. Chem. Soc.* **1953**, 2036.
(8) Clouthier, D. J.; Moule, D. C. *Topics in Current Chemistry* **1989**, *150*, 167.
(9) Moule, D. C.; Ng, K. H. K. *Can. J. Chem.* **1985**, *63*, 1378.
(10) Yakovlev, N. N.; Godunov, I. A. *Can. J. Chem.* **1992**, *70*, 931.
(11) Muñoz-Caro, C.; Niño, A.; Moule, D. C. *Chem. Phys.*, submitted for publication.
(12) Krishnan, R.; Binkley, J. S.; Seeger, R.; Pople, J. A. *J. Chem. Phys.* **1980**, *72*, 650.
(13) Schlegel, H. B. *J. Comput. Chem.* **1982**, *3*, 214.
(14) Muñoz-Caro, C.; Niño, A.; Moule, D. C. *Theor. Chim. Acta*, submitted for publication.
(15) Frisch, M. J.; Head-Gordon, M.; Trucks, G. W.; Foresman, J. B.; Schlegel, H. B.; Raghavachari, K.; Robb, M.; Binkley, J. S.; Gonzalez, C.; Defrees, D. J.; Fox, D. J.; Whiteside, R. A.; Seeger, R.; Melius, C. F.; Baker, J.; Martin, R. L.; Kahn, L. R.; Stewart, J. J. P.; Topiol, S.; Pople, J. A. *GAUSSIAN 90, Revision I*; Gaussian Inc.: Pittsburgh, PA, 1990.
(16) This G_6 nonrigid group is the same for the thioacetaldehyde molecule. The group, its operations, and the symmetry eigenvectors are detailed in: (a) Smeyers, Y. G.; Niño, A.; Moule, D. C. *J. Chem. Phys.* **1990**, *93*, 5786. (b) Moule, D. C.; Bascal, H. A.; Smeyers, Y. G.; Clouthier, D. C.; Karolczak, J.; Niño, A. *J. Chem. Phys.* **1992**, *97*, 3964.
(17) Pickett, H. M. *J. Chem. Phys.* **1972**, *56*, 1715.
(18) Harthcock, M. A.; Laane, J. *J. Phys. Chem.* **1985**, *89*, 4231.
(19) Muñoz-Caro, C.; Niño, A. *QCPE Bull.* (*program 629*) **1993**, *13*, 4.
(20) Niño, A.; Muñoz-Caro, C. *QCPE*, submitted for publication.
(21) Ozkabak, A. G.; Goodman, L. *J. Chem. Phys.* **1992**, *96*, 5958.
(22) Belov, S. P.; Tretyakov, M. Yu.; Kleiner, I.; Hougen, J. T. *J. Mol. Spectrosc.* **1993**, *160*, 61.
(23) Gu, H.; Kundu, T.; Goodman, L. *J. Phys. Chem.* **1993**, *97*, 7194.
(24) (a) Hollenstein, H.; Winther, F. *J. Mol. Spectrosc.* **1978**, *71*, 118. (b) Hollenstein, H.; Günthard, Hs. H. *Spectrochim. Acta Part A* **1971**, *27A*, 2027.
(25) Nikolova, B. *J. Mol. Struct.* **1990**, *222*, 337.
(26) Spangler, L. H.; Pratt, D. W. *J. Chem. Phys.* **1986**, *84*, 4789.
(27) Tomer, J. L.; Spangler, L. H.; Pratt, D. W. *J. Am. Chem. Soc.* **1988**, *110*, 1615.
(28) Coon, J. B.; Naugle, N. W.; McKenzie, R. D. *J. Mol. Spectrosc.* **1966**, *20*, 107.
(29) Leszczynski, J.; Goodman, L. *J. Chem. Phys.* **1993**, *99*, 4867.